Hindawi Publishing Corporation
Mathematical Problems in Engineering
Volume 2011, Article ID 783094, 18 pages
doi:10.1155/2011/783094

Research Article

An Application of Saint Venant's Theory to Volterra's Distortions

Ivana Bochicchio,[1] Ettore Laserra,[1] and Massimo Pecoraro[2]

[1] *Dipartimento di Matematica e Informatica, Università di Salerno, Via Ponte Don Melillo, I-84084 Fisciano (SA), Italy*
[2] *Dipartimento di Ingegneria dell'Informazione e Matematica Applicata, Università di Salerno, Via Ponte Don Melillo, 84084 Fisciano (SA), Italy*

Correspondence should be addressed to Ivana Bochicchio, ibochicchio@unisa.it

Received 18 November 2010; Accepted 4 December 2010

Academic Editor: Ezzat G. Bakhoum

This paper deals with the analysis of the sixth elementary Volterra's distortion for a circular hollow, homogeneous, elastic, isotropic cylinder. More precisely, the specific load connected to the sixth distortion is proved to be equivalent (in Saint Venant's theory) to a right combined compressive and bending stress and to a right combined tensile and bending stress. Our results have been applied to a material made up of steel to compare the obtained numerical results with Volterra's predictions: the values calculated through Saint Venant's theory are more strictly related to those calculated by Volterra when the cylinder thickness tends to zero.

1. Introduction

The first original and fundamental contribution to the dislocation theory was found in Weingarten's note [1], where it is shown that, in absence of external forces, equilibrium configurations for elastic bodies with nonzero internal stress can exist. Given, for example, an elastic ring initially in a natural configuration, one can create a state of deformation and, therefore of stress, by making a radial cut adding a thin slice of matter and finally soldering the two faces of the cut. The solid assumes a new equilibrium configuration (spontaneous equilibrium configuration); obviously, it is not a natural equilibrium configuration since, adding matter, nonzero internal stress can be found.

Weingarten raised the problem and indicated some concrete examples with this anomalous behavior, but he did not give analytic instruments to tackle and solve it. A fundamental contribution in this direction was given by Volterra, who used Weingarten's note as a starting point to develop a general theory. Volterra began with the observation

that Weingarten's considerations could not be validated in case of simply-connected bodies in the range of regular deformations. Hence, Volterra proposed a new theory of elastic distortions, that implied a deep revision of the mathematical theory of elasticity in the case of multiconnected domains: when in analytic structure of solutions multivalued terms appear, theorems of uniqueness cannot be valid in equilibrium problems with assigned forces [3, 7]. Note that in case of multiconnected domains, these terms, being physically admissible, cannot be discarded (as one does, in order to have uniqueness of solution, in simply-connected domains where multivalued terms have no physical meaning); hence to obtain an uniqueness theorem is not enough to assign external forces, but it is necessary to know the physically admissible multivalued properties. (The notion of distortion has been proposed by Volterra [2, 3] about one hundred years ago. The term has undergone some changes: in Love's book [4] the distortions were called dislocations. Presently, the word-combination "Volterra's distortions" is stable and identifiable: the term distortions is used for designations of phenomena creating the stress-strain state, when the external forces are absent (e.g., the inhomogeneous temperature field can create the distortion) [5, 6].)

The most general elastic distortion able to bring a right, circular, homogenous, hollow, isotropic cylinder to a state of spontaneous equilibrium, consists of six elementary distortions. For each, Volterra has tried to determine a field of displacements which fulfills the indefinite equations of elastic equilibrium and brings the body to a spontaneous equilibrium configuration. Really, Volterra was only able to determine a field of displacement that brings the cylinder to an equilibrium configuration, generating a distribution of forces globally equivalent to zero but not identically vanishing. So the problem of distortion was partially, but not totally solved. Since Volterra considered exclusively isotropic hollow cylinders, Caricato recently proposed an extension of the theory of Volterra's distortions to the case of a transversally isotropic homogeneous elastic hollow cylinder [8]; later on his findings have been reconsidered and expanded in [9]. Recently, the nonlinear aspect of distortion has been analyzed in [5, 6].

In the context of Volterra's partially results, our paper analyzes the forces induced by the sixth elementary distortion on the right circular, homogenous, hollow, isotropic cylinder with a different point of view. More precisely, exploiting Saint Venant's theory and generalizing some previous results [10, 11], we have underlined that, apart from a limited zone in the immediate vicinity of bases, the distribution of forces, considered as a specific load, can be replaced with one statically equivalent. This can be done without consequences on the effective distributions of stress and strain, and therefore, without the necessity to define the effective punctual distribution of this load acting on the bases of the cylinder.

Because of the homogeneity and isotropy of the material and of the geometric and loading symmetry of the body, we have approached the specific load as linear, constructed an auxiliary bar which has as longitudinal section the axial section of the cylinder and followed the basic considerations of Saint Venant's theory. We have found the specific load connected to the sixth distortion is equivalent (in Saint Venant's theory) to a right combined compressive and bending stress and to a right combined tensile and bending stress.

Our paper is organized as follows: in Section 2 the general theory of Volterra's distortions is briefly recalled. In Section 3 the specific load is analyzed by Saint Venant's theory. In Section 4 numerical results and their comparison with Volterra's predictions are discussed.

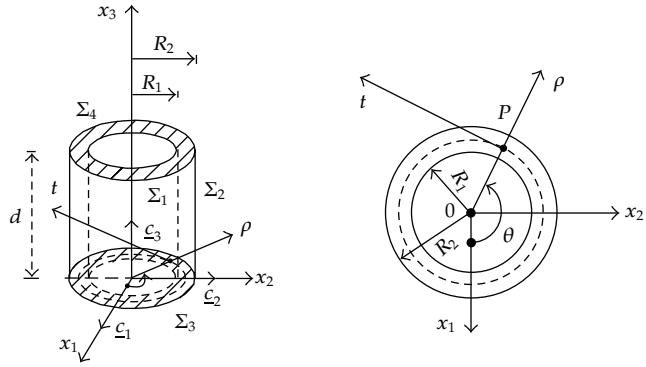

Figure 1: The hollow cylinder in the natural state and one of its cross-sections.

2. Volterra's Distortions for a Circular Hollow Cylinder

Let's consider a circular hollow (therefore doubly connected) cylinder, which is, at a certain assigned temperature, in a natural state C. This we will assume as the reference configuration. This solid is depicted in Figure 1 with one cross-section to which a generic point P belongs.

We introduce into an ordinary space a Cartesian rectangular reference $0x_1x_2x_3$ with respective versors $\{\mathbf{c}_1, \mathbf{c}_2, \mathbf{c}_3\}$ and we choose the axis $0x_3$ coinciding with the symmetry axis of the cylinder and the coordinate plane $0x_1x_2$ placed over the base. We indicate with $\rho(\mathbf{x}) = \sqrt{\mathbf{x}_1^2 + \mathbf{x}_2^2}$ and $\theta(\mathbf{x}) = \text{arc}tg(x_2/x_1)$, respectively, the distance of P from the axis of the cylinder and the anomaly.

Hereafter, we call Σ the surface of C, made from the two cylindrical coaxial surfaces Σ_1 (internal surface of radius R_1) and Σ_2 (external surface of radius R_2), and from the two bases Σ_3 (at height $x_3 = 0$) and Σ_4 (at the height $x_3 = d$).

Let $\mathbf{u}(\mathbf{x})$ be the displacement vector which is the solution of the elastic equilibrium problem for a body subjected to given external forces (without external constraints and mass forces); let us assume that $\mathbf{u}(\mathbf{x})$ includes a multivalued term related to $\theta(\mathbf{x})$. This term is physically significant in a doubly-connected region of space, as a body with hollow cylindrical symmetry.

The multivalued field of displacement $\mathbf{u}(\mathbf{x})$ has been physically interpreted by Volterra [3] in terms of the following operations: if the doubly connected cylinder is transformed into one which is simply connected by a transversal cut on an axial semiplane having the x_3 axis as edge, the vector $\mathbf{u}(\mathbf{x})$ can be characterized by a discontinuity of the first type through the semiplane of the cut. If a translatory and a rotatory displacement is imposed on one of the faces of the cut by the application, at constant temperature, of a system of external forces, a state of deformation, and therefore of stress due to the multivalued term including $\theta(\mathbf{x})$, is created into the cylinder. In order that the cylinder remains in a state of *spontaneous equilibrium* in the deformed configuration, that is, with a regular internal stress but absent of superficial forces, it is enough to reestablish the continuity remaking the cylinder doubly connected by soldering the two faces of the cut (they are soldered by adding or removing a thin slice of matter). In this way a distortion in the multiconnected body is induced.

In addition, since the rigid displacement of a face of cut with respect to the other can be obtained through a rigid translation displacement and a rigid rotation displacement, a distortion can be described by six constant parameters l, m, n, p, q, r, called *characteristic*

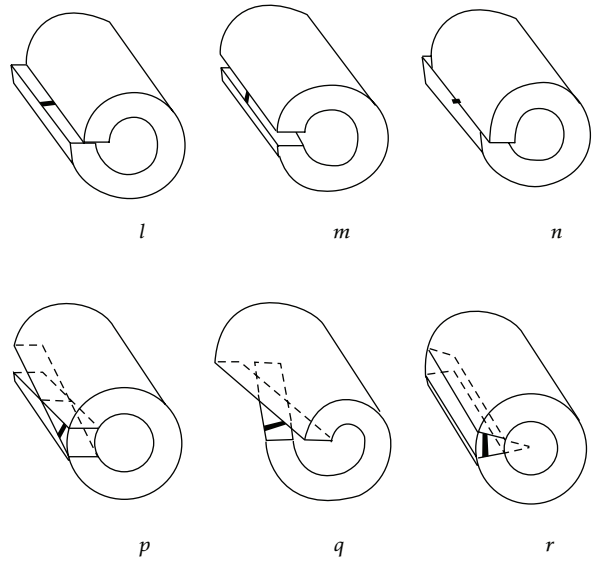

Figure 2: The six elementary Volterra's distortions.

coefficients of distortion. They correspond to the three Cartesian components of translation and rigid rotation in respect to the axes x_1, x_2, x_3. Once the characteristic coefficients are introduced, we can give the following.

Definition 2.1. Elementary distortion is the definition of the distortion that has only one of the six characteristic coefficients different from zero [3, 7, 12]. Analogously, the displacement induced by an elementary distortion has nonzero only one of the following coefficients l, m, n, p, q, r.

So making, Volterra characterized six independent distortions that are showed in Figure 2. In particular, the 6th elementary distortion is the distortion related to the coefficient r. It is realized by cutting the cylinder with an axial plane, rotating the face of the cut that faces the semiplane $x_2 < 0$ and, after adding (when $r > 0$) or removing (when $r < 0$) a thin slide of matter, soldering the sides.

Note that the axial plane of the cut can be, for example, the plane $0x_1x_3$. However, since the elementary distortion is uniquely characterized by the value of r (and not by the particular plane having the axis Ox_3 as edge), it is not essential that the plane chosen to determine the 6th elementary distortion corresponds to the coordinate plane Ox_1x_3.

2.1. Forces on the Bases: Volterra's Analysis

Volterra, after having analyzed the elastic distortion from a qualitative point of view, has partially dealt and solved the problem from a purely mathematics point of view [3]. In particular, he focused his attention on a linearly elastic, isotropic, homogeneous, doubly-connected cylinder with finite height d. The study of doubly-connected body only it is not restrictive since the analysis of multiconnected bodies requires more complex analytic problems and hence, more complex computation, but it adds nothing of conceptual interest [3].

Now, in order to briefly recall Volterra's considerations for the sixth elementary distortion, let us refer to cylindric coordinates and call (P, ρ^*, t^*, x_3^*) the counterclockwise rectangular reference system obtained by translating in P the axes ρ, t, and x_3 (see Figure 3).

More precisely, for forces acting only on the bases, the components of a displacement vector $\mathbf{u}(P)$ related to the 6th elementary distortions are [3, 4, 12–14]

$$\begin{aligned} u_{\rho^*}(\rho,\theta,x_3) &= -\frac{r}{2\pi}\rho\left[\frac{1}{2} - \frac{\mu}{2(\lambda+2\mu)}\left(\log\rho^2 - \frac{R_2^2\log R_2^2 - R_1^2\log R_1^2}{R_2^2 - R_1^2}\right)\right. \\ &\quad \left. + \frac{1}{\rho^2}\frac{\lambda+\mu}{\lambda+2\mu}R_1^2R_2^2\,\frac{\log R_2^2 - \log R_1^2}{R_2^2 - R_1^2}\right], \\ u_{t^*}(\rho,\theta,x_3) &= \frac{r}{2\pi}\rho\theta, \\ u_{x_3^*}(\rho,\theta,x_3) &= 0, \end{aligned} \tag{2.1}$$

where μ and λ are the two Lamé constants.

$\mathbf{u}(P)$ satisfies the indefinite equations of elastic equilibrium in the absence of forces of mass and generates a distribution of surface forces on the bases $\sum_3$ and $\sum_4$. In (O, ρ, θ, x_3), this distribution has the following independent from θ components (see [3, 4, 12]):

$$\begin{aligned} f_\rho(\rho,0) &= 0, \\ f_t(\rho,0) &= 0, \\ f_{x_3}(\rho,0) &= \frac{r}{2\pi}\frac{\lambda\mu}{\lambda+2\mu}\left(1 + \log\rho^2 - \frac{R_2^2\log R_2^2 - R_1^2\log R_1^2}{R_2^2 - R_1^2}\right) = -a\left[b + \log\rho^2\right]; \\ f_\rho(\rho,d) &= 0, \\ f_t(\rho,d) &= 0, \\ f_{x_3}(\rho,d) &= -\frac{r}{2\pi}\frac{\lambda\mu}{\lambda+2\mu}\left(1 + \log\rho^2 - \frac{R_2^2\log R_2^2 - R_1^2\log R_1^2}{R_2^2 - R_1^2}\right) = a\left[b + \log\rho^2\right], \end{aligned} \tag{2.2}$$

where

$$\begin{aligned} a &= -\frac{r}{2\pi}\frac{\lambda\mu}{\lambda+2\mu}, \\ b &= 1 - \frac{R_2^2\log R_2^2 - R_1^2\log R_1^2}{R_2^2 - R_1^2}. \end{aligned} \tag{2.3}$$

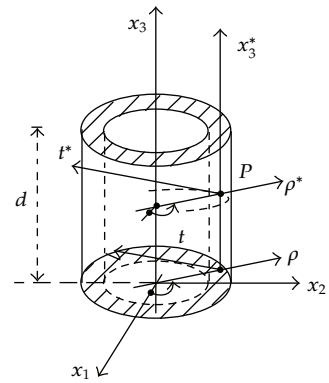

Figure 3: Hollow cylinder referred to Cartesian and cylindrical reference system.

3. Analysis of the Specific Load as Characteristic of the External Solicitation

In this section, we will analyze the solution of the elastic equilibrium proposed by Saint Venant for a prismatic isotropic homogeneous linearly elastic solid subjected to a specific load on the bases.

In Saint Venant's theory one can replace the specific load with an equivalent one. In this way, apart from a thin zone near the bases, called *extinction zone*, we have no consequences on the effective distribution of stress and strain. So, every solution of the problem of the elastic equilibrium can be considered as a solution of an infinity of cases which are pertinent to an infinity of load models, distributed with different laws, but having the same resultant. This resultant can be replaced, as we know from static, by a force through a generic point P' belonging to the base section, and by a couple that has, in respect to P', the same moment of the resultant. Note that the resultant is applied in a suitable point, generally different from P'.

Since the force and the couple can be decomposed with respect to the three axes of the reference system, the six *characteristics of the external solicitation*, that is, the three components of the force and of the couple, are individuated.

Hence, since these characteristics completely define every system of external loads acting on the bases of the solid, it is unnecessary to define their effective punctual distributions. As a consequence, the more general case can be solved through a linear combination of six elementary cases: normal stress, shear stress along x_2, shear stress along x_1, bending moment around x_1, bending moment around x_2, and torsional moment.

3.1. Saint Venant's Theory to Analyze the Sixth Elementary Distortion

This section deals with the analysis the specific load in Saint Venant's theory (see [10, 11, 15]). Hereafter, we will assume that the hollow cylinder is thin (i.e., its thickness $\Delta\rho = R_2 - R_1$ is small with respect to the radius R_1) and we will consider just the vertical component of the load, that is, $f_{x_3}(\rho, d)$, acting on the base $x_3 = d$. It is clear that, for the equilibrium, the vertical component acting on the inferior base $x_3 = 0$, will be directly opposed.

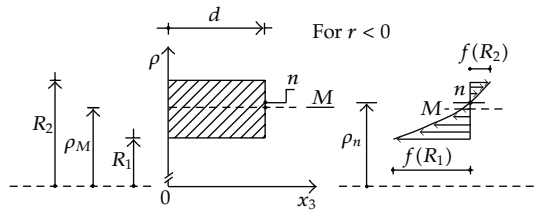

Figure 4: Specific load distribution.

$f_{x_3}(\rho, d)$ can be simply denoted with $f(\rho)$, since, once x_3 is fixed, it is a function of ρ only. Moreover, since $f(\rho)$ is monotone in $[R_1, R_2]$, the equation $f(\rho) = 0$ has in (R_1, R_2) one real root:

$$\rho_n = \sqrt{e^{(R_2^2 \log R_2^2 - R_1^2 \log R_1^2)/(R_2^2 - R_1^2) - 1}}. \tag{3.1}$$

In other words, ρ_n is the value or the radius of the cylindrical neutral surface of the hollow body with respect to the specific load.

Note that in every axial section, since the deformed hollow cylinder has stretched and compressed bending fibres to conserve its original volume, $R_1 < \rho_n < R_2$ must be verified. In addition (see [3, page 435] and Figure 4)

$$\rho_M < \rho_n < R_2, \tag{3.2}$$

where

$$R_M = \rho_M = \frac{R_1 + R_2}{2}. \tag{3.3}$$

Now, let us consider a simply connected auxiliary rectangular beam. We suppose that it has height d (i.e., the same height of the cylinder) and cross-section with unitary base for convenience. More precisely, we suppose that the cross-section of the auxiliary beam is a rectangle whose area is $(R_2 - R_1) * 1$ and if we consider an axial section of the cylinder of height d, then it can be assimilated to a longitudinal section of the auxiliary beam.

Moreover, the auxiliary beam is subjected to the load $f(\rho)$ on the bases.

With reference to the aforementioned beam, from (3.2) we obtain that, in modulus, the area delimited by $f(\rho)$ on $[R_1, \rho_n]$ is greater than that delimited on $[\rho_n, R_2]$:

$$\left| \int_{R_1}^{\rho_n} f(\rho) d\rho \right| > \left| \int_{\rho_n}^{R_2} f(\rho) d\rho \right|. \tag{3.4}$$

Now, we would like to analyze the two zones delimitated by ρ_n (see Figure 4) and separately study the distribution of load.

More precisely, since in Saint Venant's theory it is unnecessary to define the effective punctual distribution of the load on the bases of the body, we will appropriately reduce the

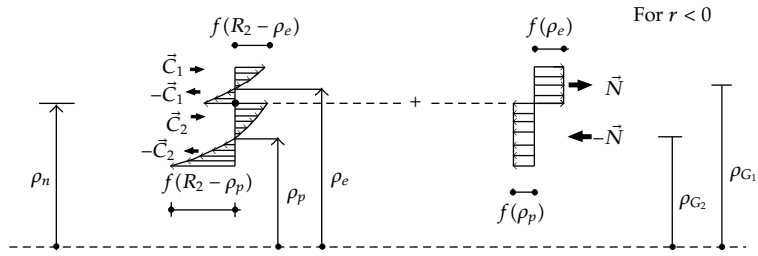

Figure 5: Decomposition of the specific load.

load induced in each section by the sixth elementary distortion to a normal stress and to a couple.

The normal stress and the momentum of the couple, both applied in the barycenter of the section, will have a fundamental role in our analysis; more precisely, they allow us to prove the specific load connected to the sixth distortion is equivalent (in Saint Venant's theory) to a right combined compressive and bending stress and to a right combined tensile and bending stress. These ideas will be developed in detail in the following sections.

3.1.1. Upper Section: $\rho \in [\rho_n, R_2]$

Let's focus our attention on $\rho \in [\rho_n, R_2]$; let ρ_e be the value of ρ where we have to translate the diagram of $f(\rho)$ to divide the upper section in two with, in modulus, the same area (see Figure 5).

The explicit value of ρ_e is obtained by solving the following equation:

$$\int_{\rho_n}^{\rho_e} [f(\rho) - f(\rho_e)]\, d\rho + \int_{\rho_e}^{R_2} [f(\rho) - f(\rho_e)]\, d\rho = 0, \tag{3.5}$$

from which we easily derive

$$\rho_e = \sqrt{e^{-(2R_2 - 2\rho_n - R_2 \log R_2^2 + \rho_n \log \rho_n^2)/(R_2 - \rho_n)}}. \tag{3.6}$$

As already underlined, the specific load acting on the section can be represented by a normal stress **N** applied on the barycenter G_1 of the section whose modulus is

$$N = f(\rho_e)(R_2 - \rho_n) = a(R_2 - \rho_n)\left(b + \log \rho_e^2\right), \tag{3.7}$$

and by a couple $(\mathbf{C}_1, -\mathbf{C}_1)$, whose vectors are applied in $G_1^{(1)}$ and $G_1^{(2)}$, respectively, that is, in the barycenters of the two sections having the same area (see Figure 5).

So, in order to evaluate the couple, its arm and the coordinate of its center, we want to specify the positions of these barycenters.

More precisely, using the technique of static momenta, we compute the values of ρ corresponding to the two barycenters; so, by the formula

$$\rho_{G_1^{(1)}} = \frac{\int_{\rho_e}^{R_2} \rho[f(\rho) - f(\rho_e)]\,d\rho}{\int_{\rho_e}^{R_2} [f(\rho) - f(\rho_e)]\,d\rho}, \tag{3.8}$$

we have

$$\rho_{G_1^{(1)}} = \frac{R_2^2 - \rho_e^2 - 2R_2^2(\log R_2 - \log \rho_e)}{4[R_2 - \rho_e - R_2(\log R_2 - \log \rho_e)]}, \tag{3.9}$$

while

$$\rho_{G_1^{(2)}} = \frac{\rho_e^2 - \rho_n^2 - 2\rho_n^2(\log \rho_e - \log \rho_n)}{4[\rho_e - \rho_n - \rho_n(\log \rho_e - \log \rho_n)]}, \tag{3.10}$$

obtained by the analogous formula

$$\rho_{G_1^{(2)}} = \frac{\int_{\rho_n}^{\rho_e} \rho[f(\rho) - f(\rho_e)]\,d\rho}{\int_{\rho_n}^{\rho_e} [f(\rho) - f(\rho_e)]\,d\rho}. \tag{3.11}$$

Moreover, referring to the area

$$\int_{\rho_e}^{R_2} [f(\rho) - f(\rho_e)]\,d\rho, \tag{3.12}$$

it is possible to evaluate the modulus of the vector $\mathbf{C}_1$

$$C_1 = a\left[2(R_2 - \rho_e) - R_2\left(\log R_2^2 - \log \rho_e^2\right)\right]. \tag{3.13}$$

It is clear that, referring to the area $\int_{\rho_n}^{\rho_e} [f(\rho) - f(\rho_e)]\,d\rho$, when we evaluate the modulus of the second vector of the couple it is equal to $a[2\rho_e - 2\rho_n - \rho_n(\log \rho_e^2 - \log \rho_n^2)]$. Note that since the evaluated areas are equal, this vector can be called $-\mathbf{C}_1$.

As the vectors of the couple are applied in the barycenter of the two equivalent sections, its arm is $b_1 = (\rho_{G_1^{(1)}} - \rho_{G_1^{(2)}})$, the coordinate of its center D_1 is $\rho_{D_1} = (\rho_{G_1^{(1)}} + \rho_{G_1^{(2)}})/2$, and its momentum $\mathbf{M}_{D_1}$ has, in modulus, the following expression:

$$M_{D_1} = b_1 C_1 = a\left(\rho_{G_1^{(1)}} - \rho_{G_1^{(2)}}\right)\left[2R_2 - 2\rho_e - R_2\left(\log R_2^2 - \log \rho_e^2\right)\right]. \tag{3.14}$$

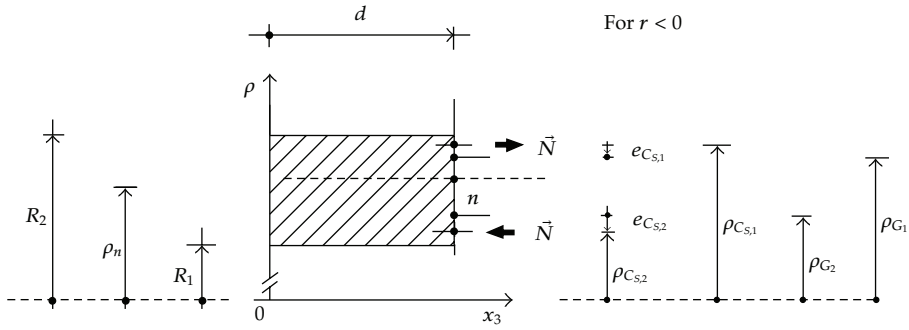

Figure 6: Centers of stress and their positions.

In order to obtain the load globally acting on the section (normal stress and momentum of the couple both applied in the same point, i.e., in D_1), we need to translate $\mathbf{N}$ in D_1 and hence evaluate, in modulus, the momentum $\mathbf{M}'_{D_1}$ related to this translation:

$$\begin{aligned} M'_{D_1} &= (\rho_{G_1} - \rho_{D_1}) f(\rho_e)(R_2 - \rho_n) \\ &= a\left[b + \log \rho_e^2\right](R_2 - \rho_n)\left[\frac{R_2 + \rho_n}{2} - \frac{\left(\rho_{G_1^{(1)}} + \rho_{G_1^{(2)}}\right)}{2}\right]. \end{aligned} \tag{3.15}$$

So, the total momentum applied in D_1 is

$$\begin{aligned} M''_{D_1} &= M'_{D_1} + M_{D_1} \\ &= \frac{1}{2} a(R_2 - \rho_n)\left(\rho_n - \rho_{G_1^{(1)}} - \rho_{G_1^{(2)}} + R_2\right)\left(b + \log \rho_e^2\right) \\ &\quad - a\left(\rho_{G_1^{(1)}} - \rho_{G_1^{(2)}}\right)\left[2R_2 - 2\rho_e - R_2\left(\log R_2^2 - \log \rho_e^2\right)\right]. \end{aligned} \tag{3.16}$$

Note that the center D_1 does not coincide with the barycenter of the section:

$$\rho_{D_1} < \rho_{G_1} = \frac{R_2 + \rho_n}{2}. \tag{3.17}$$

Because of this limitation and the sign of $\mathbf{N}$, $\mathbf{M}'_{D_1}$, and $\mathbf{M}_{D_1}$ have opposite signs. Moreover, M''_{D_1} is less then M_{D_1}, but has its sign.

Once the explicit form of M''_{D_1} is known, we can compute the eccentricity $e_{C_{S,1}}$ of the normal stress $\mathbf{N}$ with respect to the point D_1 (see Figure 6), and hence, the position of the center of stress $C_{S,1}$. Note that $C_{S,1}$ characterizes the point belonging to the meridian plane (that is also plane of stress) where one can apply only the normal stress to obtain the same

effect produced by the specific load acting on the bases of the cross-section of the auxiliary beam. More precisely, in the coordinate-plane $(0, \rho, x_3)$,

$$\rho_{C_{S,1}} = e_{C_{S,1}} + \rho_{D_1} = \frac{M''_{D_1}}{N} + \frac{1}{2}\left(\rho_{G_1^{(1)}} + \rho_{G_1^{(2)}}\right). \tag{3.18}$$

Finally, since Saint Venant's theory refers to the barycenter, we have to evaluate the momentum $\mathbf{M}_{G_1}$ of $\mathbf{N}$ with respect to G_1. So, letting

$$b'_1 = \rho_{C_{S,1}} - \rho_{G_1} = -\frac{\left(\rho_{G_1^{(1)}} - \rho_{G_1^{(2)}}\right)\left[2R_2 - 2\rho_e - R_2\left(\log R_2^2 - \log \rho_e^2\right)\right]}{\left(R_2 - \rho_n\right)\left(b + \log \rho_e^2\right)} \tag{3.19}$$

be the arm, we have

$$M_{G_1} = b'_1 N = -a\left(\rho_{G_1^{(1)}} - \rho_{G_1^{(2)}}\right)\left[2R_2 - 2\rho_e - R_2\left(\log R_2^2 - \log \rho_e^2\right)\right]. \tag{3.20}$$

Then, in agreement with Saint Venant's theory, for all $z \in [0, d]$ in the section there is the action of the following linear $\sigma_{x_3}^{(1)}(\rho)$ (right combined tensile and bending stress):

$$\begin{aligned}
\sigma_{x_3}^{(1)}(\rho) &= \frac{N}{L_1} + \frac{M_{G_1}}{I_{G_1}}\left(\rho - \frac{R_2 + \rho_n}{2}\right) \\
&= f(\rho_e) - \frac{12a\left(\rho_{G_1^{(1)}} - \rho_{G_1^{(2)}}\right)\left[2R_2 - 2\rho_e - R_2\left(\log R_2^2 - \log \rho_e^2\right)\right]}{\left(R_2 - \rho_n\right)^3}\left(\rho - \frac{R_2 + \rho_n}{2}\right) \\
&= a\left(b + \log \rho_e^2\right) + \\
&\quad - \frac{12a\left(\rho_{G_1^{(1)}} - \rho_{G_1^{(2)}}\right)\left[2R_2 - 2\rho_e - R_2\left(\log R_2^2 - \log \rho_e^2\right)\right]}{\left(R_2 - \rho_n\right)^3}\left(\rho - \frac{R_2 + \rho_n}{2}\right).
\end{aligned} \tag{3.21}$$

Actually, L_1 is reduced to $R_2 - \rho_n$ since the cross-section of the bar has unitary bases; moreover, $I_{G_1} = (1/12)(R_2 - \rho_n)^3$, as it is known, is the momentum of inertia in respect to an axis through G_1 and parallel to the bases of the same cross-section.

3.1.2. Lower Section: $\rho \in [R_1, \rho_n]$

Let's consider the lower section where $\rho \in [R_1, \rho_n]$. In order to obtain, in Saint Venant's theory, the explicit form of the stress acting on the bases of the auxiliary beam, we briefly recall the same strategy amply described in the previous case. So

$$\rho_p = \sqrt{e^{-(2\rho_n - 2R_1 - \rho_n \log \rho_n^2 + R_1 \log R_1^2)/(\rho_n - R_1)}} \tag{3.22}$$

is the point where we have to translate the diagram of $f(\rho)$ to obtain the division of the lower section into two smaller ones with, in modulus, the same area. The normal stress applied to the barycenter G_2 of the section, whose $\rho_{G_2} = (\rho_n + R_1)/2$, is in modulus

$$N = f(\rho_p)(\rho_n - R_1) = a(\rho_n - R_1)\left(b + \log \rho_p^2\right). \tag{3.23}$$

Moreover, we can evaluate the couple $(\mathbf{C}_2, -\mathbf{C}_2)$

$$C_2 = a\left[2(\rho_n - \rho_p) - \rho_n\left(\log \rho_n^2 - \log \rho_p^2\right)\right], \tag{3.24}$$

its arm

$$\begin{aligned} b_2 &= \rho_{G_2^{(1)}} - \rho_{G_2^{(2)}} \\ &= \frac{\rho_n^2 - \rho_p^2 - 2\rho_n^2(\log \rho_n - \log \rho_p)}{4[\rho_n - \rho_p - \rho_n(\log \rho_n - \log \rho_p)]} - \frac{\rho_p^2 - R_1^2 - 2R_1^2(\log \rho_p - \log R_1)}{4[\rho_p - R_1 - R_1(\log \rho_p - \log R_1)]}, \end{aligned} \tag{3.25}$$

and clearly the coordinate of its center D_2

$$\rho_{D_2} = \frac{\rho_{G_2^{(1)}} + \rho_{G_2^{(2)}}}{2}. \tag{3.26}$$

Following the same line of reasoning, we can consider

$$\begin{aligned} M''_{D_2} = {} & \frac{1}{2}a(\rho_n - R_1)\left(\rho_n - \rho_{G_2^{(2)}} - \rho_{G_2^{(1)}} + R_1\right)\left(b + \log \rho_p^2\right) \\ & - a\left(\rho_{G_2^{(1)}} - \rho_{G_2^{(2)}}\right)\left[2\rho_n - 2\rho_p - \rho_n\left(\log \rho_n^2 - \log \rho_p^2\right)\right], \end{aligned} \tag{3.27}$$

and hence

$$\rho_{C_{S,2}} = e_{C_{S,2}} + \rho_{D_2} = \frac{M''_{D_2}}{N} + \frac{1}{2}\left(\rho_{G_2^{(1)}} + \rho_{G_2^{(2)}}\right). \tag{3.28}$$

Finally, since Saint Venant's theory refers to the barycenter, we have to evaluate the momentum $\mathbf{M}_{G_2}$ of $\mathbf{N}$ with respect to G_2. So, letting

$$b'_2 = -\frac{\left(\rho_{G_2^{(1)}} - \rho_{G_2^{(2)}}\right)\left[2\rho_n - 2\rho_p - \rho_n\left(\log \rho_n^2 - \log \rho_p^2\right)\right]}{(\rho_n - R_1)\left(b + \log \rho_p^2\right)} \tag{3.29}$$

be the arm, we have

$$M_{G_2} = -a\left(\rho_{G_2^{(1)}} - \rho_{G_2^{(2)}}\right)\left[2\rho_n - 2\rho_p - \rho_n\left(\log\rho_n^2 - \log\rho_p^2\right)\right]. \tag{3.30}$$

Thus, in agreement with Saint Venant's theory, for all $z \in [0, d]$ in the section there is the action of the following linear $\sigma_{x_3}^{(2)}(\rho)$ (right combined compressive and bending stress):

$$\begin{aligned}\sigma_{x_3}^{(2)}(\rho) &= \frac{N}{L_2} + \frac{M_{G_2}}{I_{G_2}}\left(\rho - \frac{R_1 + \rho_n}{2}\right) \\ &= a\left(b + \log\rho_p^2\right) - \frac{12a\left(\rho_{G_2^{(1)}} - \rho_{G_2^{(2)}}\right)\left[2\rho_n - 2\rho_p - \rho_n\left(\log\rho_n^2 - \log\rho_p^2\right)\right]}{\left(\rho_n - R_1\right)^3}\left(\rho - \frac{R_1 + \rho_n}{2}\right).\end{aligned} \tag{3.31}$$

Actually, L_2 is reduced to $\rho_n - R_1$ since the cross-section of the bar has unitary bases; moreover, $I_{G_2} = (1/12)(\rho_n - R_1)^3$, as it is known, is the momentum of inertia in respect to an axis through G_2 and parallel to the bases of the same cross-section.

4. Numerical Results

The importance of Saint Venant's theory applied to the sixth elementary distortions is mainly based on the information content of (3.21) and (3.31). More precisely, they underline what kind of load is induced (in Saint Venant's theory) by the sixth elementary distortion: it is a right combined tensile and bending stress and a right combined compressive and bending stress. Hence, for every axial section it is possible to evaluate the tensional state with the well-known Saint Venant's formulas [15].

However, in order to apply Saint Venant's theory, our analysis has required some assumptions: we have considered a suitable auxiliary beam and we have assumed that the load on the bases has a linear diagram. So, to evaluate the deviation of our results from Volterra's predictions, in this section we compare (3.21) and (3.31) with $f_{x_3}(\rho)$ computed by Volterra.

More precisely, let us consider the cylinder made of steel, for which

$$\lambda = 1.53 * 10^{-6}\,\mathrm{kg/cm^2}, \qquad \nu = 7.89 * 10^{5}\,\mathrm{kg/cm^2}, \tag{4.1}$$

and let us subject the side of the cut to this rotation $r = -1.62 * 10^{-5}$ rad.

The smallness of the chosen angle is justified by the required thickness of the cylinder, by the material it is made of and by the hypothesis that Saint Venant's theory is valid for small displacements.

Moreover, we fixed $R_2 = 4$ cm and then we examined the following two cases:

$$\beta = \frac{R_1}{R_2} = 0.5, \qquad \beta = \frac{R_1}{R_2} = 0.9 \tag{4.2}$$

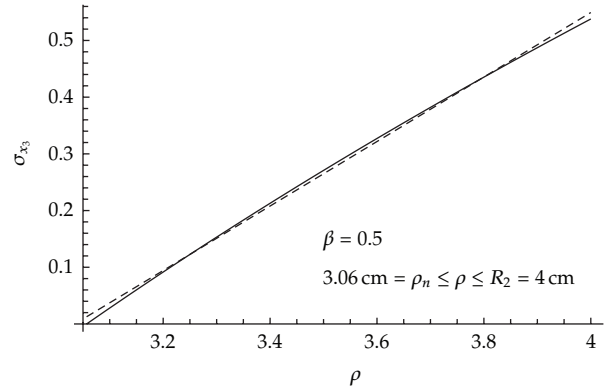

Figure 7: Load in Volterra's theory (black) and load in our results (dashed) for $\beta = 0.5$. The picture refers to the upper section, that is, 3.06 cm = $\rho_n \le \rho \le R_2 = 4$ cm.

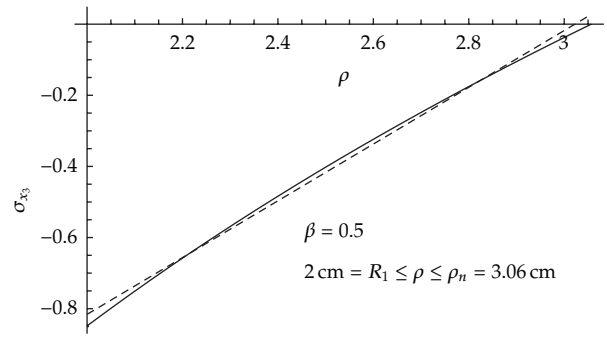

Figure 8: Load in Volterra's theory (black) and load in our results (dashed) for $\beta = 0.5$. The picture refers to the lower section, that is, 2 cm = $R_1 \le \rho \le \rho_n$ = 3.06 cm.

from which

$$R_1 = 2\,\text{cm}, \quad \Delta R = 2\,\text{cm}, \qquad R_1 = 3.6\,\text{cm}, \quad \Delta R = 0.4\,\text{cm}. \tag{4.3}$$

When $\beta = 0.5$, in Figures 7 and 8, we have shown the graphics of the different loads. These pictures clearly demonstrate that the dashed line (expression of load in our results) is a good approximation of Volterra's prediction. The percent deviation of our result from Volterra's formula, for different values of ρ, is shown in Figures 9 and 10. This deviation is calculated dividing the difference between the load in Volterra's theory and the load in our results by the load in Volterra's theory. As already underlined in the analytic treatment of the previous section, apart from a small zone near the neutral axis this deviation is "small": the "error" made in such approximation can be strongly controlled.

Note that it is not restrictive to consider a small set of fixed ρ as to compute this deviation. In fact, apart from a small zone near the neutral axis, which thickness, in both cases, does not exceed the 16% of the thickness of the considered section, this deviation remains bounded by the same small value. Analyzing Figures 9 and 10, it seems that this value is about 5.

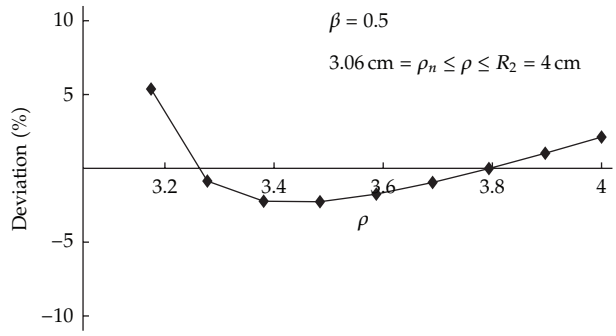

Figure 9: Graphic representation of the percent deviation of our results from Volterra's prediction for $\beta = 0.5$ and 3.06 cm = $\rho_n \le \rho \le R_2$ = 4 cm.

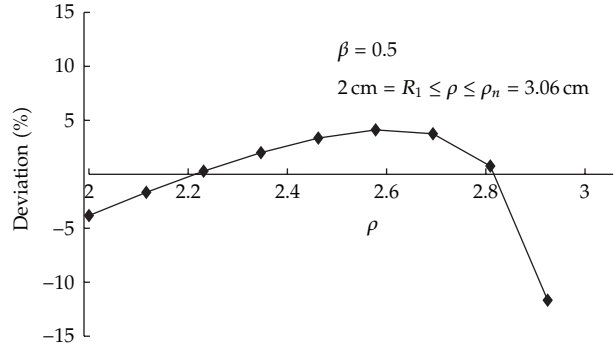

Figure 10: Graphic representation of the percent deviation of our results from Volterra's prediction for $\beta = 0.5$ and 2 cm = $R_1 \le \rho \le \rho_n$ = 3.06 cm.

We want to underline that since $f_{x_3}(\rho)$ tends to zero in this small zone near the neutral axis, the aforementioned formula is unable to give us information on the percent deviation, that by Figures 7 and 8 is bounded.

Finally, we have compared the obtained numerical results with Volterra's prediction for a very thin cylinder. More precisely, when $\beta = 0.9$, that is, when that R_1 differs little from R_2, in Figures 11 and 12 we have shown the graphics of the different loads. In this case it is rather impossible to distinguish between them. Clearly (see Figures 13 and 14), apart from a small zone near the neutral axis, which thickness, in both cases, does not exceed the 16% of the thickness of the considered section, the deviation is also strongly bounded (about by 0.6 per cent).

We can conclude by seeing that the values calculated through Saint Venant's theory are more strictly related to those calculated by Volterra when the cylinder thickness tends to zero.

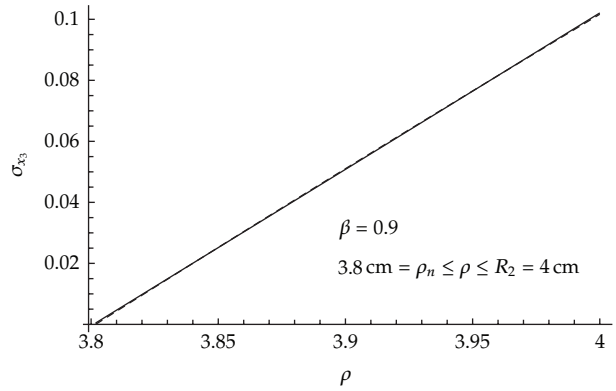

Figure 11: Load in Volterra's theory (black) and load in our results (dashed) for $\beta = 0.9$. The picture refers to the upper section, that is, $3.8\,\text{cm} = \rho_n \leq \rho \leq R_2 = 4\,\text{cm}$. Note that the two lines are indistinguishable.

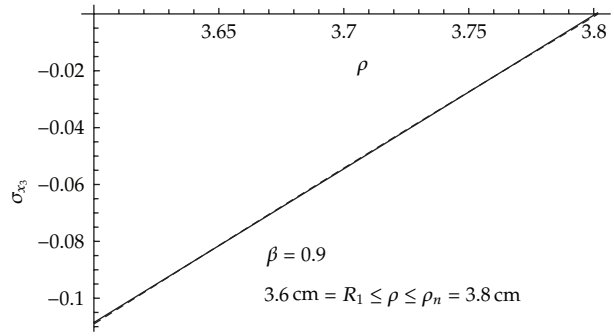

Figure 12: Load in Volterra's theory (black) and load in our results (dashed) for $\beta = 0.9$. The picture refers to the lower section, that is, $3.6\,\text{cm} = R_1 \leq \rho \leq \rho_n = 3.8\,\text{cm}$. Note that the two lines are indistinguishable.

5. Conclusions

In this paper we have improved Volterra's analysis focusing our attention on the load induced on the bases by one of the six elementary distortions, the sixth one. Precisely, taking advantage from the Saint Venant theory, tackled for our case, we have evaluated the nature of this force. In particular, approaching the specific load as linear one and constructing an auxiliary bar which has as longitudinal section the axial section of the cylinder, we have analyzed the tensional state with the well known Saint Venant's principle.

We have obtained the specific load connected to the sixth distortion is equivalent (in Saint Venant's theory) to a right combined compressive and bending stress and to a right combined tensile and bending stress.

As previously underlined, this result is achieved by considering some assumptions and approximations. So, to evaluate its reliability and precision, we have added numerical simulations able to visualize, and hence compare, the load given by Volterra and the load computed through the Saint Venant's theory. The numerical analysis, applied to a thin steel cylinder, demonstrates that we have obtained a good approximations of Volterra's prediction: in all the analyzed cases, apart from the *extinction zone*, the deviation between the two expression of the same load remains strongly bounded. This gives reason to a possible

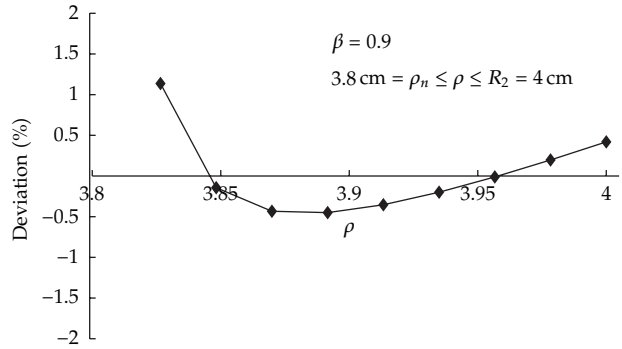

Figure 13: Graphic representation of the percent deviation of our results from Volterra's prediction for $\beta = 0.9$ and 3.8 cm = $\rho_n \le \rho \le R_2$ = 4 cm.

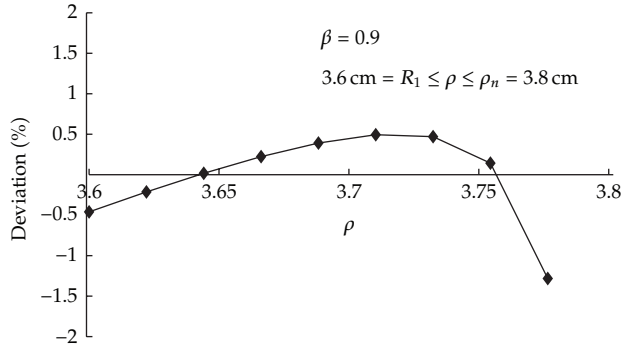

Figure 14: Graphic representation of the percent deviation of our results from Volterra's prediction for $\beta = 0.9$ and 3.6 cm = $R_1 \le \rho \le \rho_n$ = 3.8 cm.

generalization of the statement. More precisely, we stress that the various results obtained here are limited to the analysis of the sixth elementary distortion. As an interesting research perspective, we aim to address the generalization of our analysis to the case of a general distortion as we are planning for forthcoming investigations.

References

[1] M. Weingarten, "Sur les surfaces de discontinuité dans la théorie des corps solids," *Rend. Accad. Lincei*, vol. 10, pp. 57–60, 1901.
[2] V. Volterra, "Sulle distorsioni dei corpi elastici simmetrici," *Rend. Accad. Lincei*, vol. 14, 1905.
[3] V. Volterra, *L'equilibre des corps élastique multiplement connexes*, Gauthier-Villars, Imprimeur-libraire, Paris, France, 1907.
[4] A. E. H. Love, *The Mathematical Theory of Elasticity*, Cambridge Univerity Press, Cambridge, UK, 4th edition, 1952.
[5] C. Cattani and J. Rushchitsky, "Volterra's distortions in nonlinear hyperelastic media," *International Journal of Applied Mathematics and Mechanics*, vol. 3, pp. 14–34, 2005.
[6] L. M. Zubov, *Nonlinear Theory of Dislocations and Disclinations in Elastic Bodies*, vol. 47 of *Lecture Notes in Physics. New Series m: Monographs*, Springer, Berlin, Germany, 1997.

[7] G. Grioli, "Vito Volterra's work on elastic distortions," in *International Conference in Memory of Vito Volterra*, vol. 92 of *Atti Convegni Lincei*, pp. 271–289, Accad. Naz. Lincei, Rome, Italy, 1992.
[8] G. Caricato, "On the Volterra's distortions theory," *Meccanica*, vol. 35, pp. 411–420, 2000.
[9] E. Laserra and M. Pecoraro, "Volterra's theory of elastic dislocations for a transversally isotropic homogeneous hollow cylinder," *Nonlinear Oscillations*, vol. 6, no. 1, pp. 56–73, 2003.
[10] I. Bochicchio, E. Laserra, and M. Pecoraro, "Sulla sesta distorsione elementare di Volterra per un cilindro cavo omogeneo e isotropo di altezza finita con carico alla Saint Venant," *Atti dell' Accademia Peloritana dei Pericolanti, Classe di Scienze Fisiche, Matematiche e Naturali*, vol. 86, no. 1, Article ID C1A0801003, 2008.
[11] I. Bochicchio, E. Laserra, and M. Pecoraro, "Sul Carico alla De Saint Venant della Sesta Distorsione Elementare di Volterra," in *Math. Phys. Mod. Eng. Sciences, Societá nazionale di scienze letterarie e arti in Napoli, Studi in onore di Pasquale Renno*, pp. 9–15, Liguori Editore, 2008.
[12] A. Signorini, *Lezioni di Fisica Matematica*, Libreria Eredi Virgilio Veschi, Roma, Italy, 1953.
[13] A. I. Lurie, *Theory of Elasticity*, Springer, Berlin, Germany, 2005.
[14] P. Villaggio, *Mathematical Models for Elastic Structures*, Cambridge University Press, Cambridge, UK, 1997.
[15] D. Iesan, *Saint-Venant's Problem*, Springer, Berlin, Germany, 2008.